Check for updates

Analysis and Modifications of Turbulence Models for Wind Turbine Wake Simulations in Atmospheric Boundary Layers

Enrico G. A. Antonini
Department of Mechanical
and Industrial Engineering,
University of Toronto,
Toronto, ON M5S 3G8, Canada
e-mail: enrico.antonini@mail.utoronto.ca

David A. Romero
Department of Mechanical
and Industrial Engineering,
University of Toronto,
Toronto, ON M5S 3G8, Canada
e-mail: d.romero@utoronto.ca

Cristina H. Amon
Professor
Department of Mechanical
and Industrial Engineering,
University of Toronto,
Toronto, ON M5S 3G8, Canada
e-mail: cristina.amon@utoronto.ca

Computational fluid dynamics (CFD) simulations of wind turbine wakes are strongly influenced by the choice of the turbulence model used to close the Reynolds-averaged Navier-Stokes (RANS) equations. A wrong choice can lead to incorrect predictions of the velocity field characterizing the wind turbine wake and, consequently, to an incorrect power estimation for wind turbines operating downstream. This study aims to investigate the influence of different turbulence models, namely the k–ε, k–ω, SSTk–ω, and Reynolds stress models (RSM), on the results of CFD wind turbine simulations. Their influence was evaluated by comparing the CFD results with the publicly available experimental measurements of the velocity field and turbulence quantities from the Sexbierum and Nibe wind farms. Consistent turbulence model constants were proposed for atmospheric boundary layer (ABL) and wake flows according to previous literature and appropriate experimental observations, and modifications of the derived turbulence model constants were also investigated in order to improve agreement with experimental data. The results showed that the simulations using the k–ε and k–ω turbulence models consistently overestimated the velocity and turbulence quantities in the wind turbine wakes, whereas the simulations using the shear-stress transport (SST) k–ω and RSMs could accurately match the experimental data. Results also showed that the predictions from the k–ε and k–ω turbulence models could be improved by using the modified set of turbulence coefficients.
[DOI: 10.1115/1.4039377]

Downloaded from http://asmedigitalcollection.asme.org/solarenergyengineering/article-pdf/140/3/031007/6330434/sol_140_03_031007.pdf by Stanford University user on 16 August 2021

1 Introduction

The increasing global energy demand, combined with depletion of fossil–fuel reserves and stricter environmental regulations, has led to the development of alternative energy solutions like wind energy. In the last twenty years, the global installed wind capacity has been experiencing an exponential growth, reaching approximately 430 GW at the end of 2015 [1]. This growth in the wind energy sector has brought about the installation of large wind farms, which are spreading in many countries as an important source of energy competitive with traditional fossil–fuel power stations. As a consequence, the focus of wind engineers has shifted from the improvement of single wind turbines in the early stage of the wind energy development to the optimal design and operation of clusters of turbines, i.e., wind farms.

One important phenomenon that has to be investigated with regard to wind farms is the wake generated by wind turbines, which lowers the wind speed experience by the turbines placed downstream and, as a consequence, reduces their power production [2]. Accurate modeling of wake effects is therefore crucial for a correct estimation of the annual energy production and for an optimal design of the wind turbines placement. Different approaches exist to model wind turbine wakes, namely analytical and numerical models [3]. Whereas analytical wake models have the advantage of being simple and computationally efficient, numerical models, which rely on computational fluid dynamics (CFD), offer higher accuracy and flexibility to handle different ambient conditions.

Contributed by the Solar Energy Division of ASME for publication in the Journal of Solar Energy Engineering: Including Wind Energy and Building Energy Conservation. Manuscript received January 9, 2017; final manuscript received February 13, 2018; published online March 13, 2018. Assoc. Editor: Douglas Cairns.

In recent years, the use of CFD wake models in wind farm investigations has been undergoing a rapid growth thanks to improvements of computational technologies and resources. The first CFD study dates back to 1985, when Crespo et al. [4] developed a CFD code to analyze the wake of wind turbines in the atmospheric surface layer. Since then, especially in the last 15 years, many works have been proposed in literature that covered numerical, modeling, and accuracy issues of CFD wind turbine simulations [5].

A significant part of CFD models uses the Reynolds-averaged Navier-Stokes (RANS) equations to solve the flow field. RANS equations are based on a time-averaging procedure for the flow flied solution and require additional turbulence modeling to close the system of equations. Different turbulence models have been tested in wind turbine simulations to predict wake velocities and power output when the actuator disk technique is used to simulate the wind turbines. One of the most used turbulence models is the k–ε model, which found implementation in many works, among which the most notable are Refs. [6–8]. The results of the simulations using the k–ε model showed quite good agreement with experimental measurements when the CFD codes used the parabolic RANS equations (i.e., the pressure gradient is neglected and the velocity profile is prescribed behind the wind turbine), whereas the agreement was poor when the full RANS equations was employed (elliptic equations). This limitation was first observed by Réthoré [7], who suggested that the cause may lie in the limited validity of the eddy viscosity assumption (Boussinesq approximation) in the near-wake region. Another turbulence model widely used is the k–ω model, whose most notable implementations were conducted by Prospathopoulos et al. [9,10]. Similarly to the k–ε model, the results of the simulations using the k–ω model showed poor agreement with experimental observations. A different approach that does not make use of the Boussinesq

 Copyright © 2018 by ASME

hypothesis and computes directly the Reynolds stresses is the Reynolds stress model (RSM), which was tested by Cabezón et al. [8] in comparison with the standard k–ε model. One of the most promising turbulence models, the shear-stress transport (SST) k–ω model, widely used in aeronautical applications, is still missing from the literature about wind turbine simulations.

Due to the aforementioned limitations, several authors have proposed modifications of the original models to improve agreement with experimental data. El Kasmi and Masson [11] modified the k–ε model adding a source term to the transport equation for the turbulent energy dissipation in a region in close proximity to the rotor. Another modified version is the realizable k–ε model, which was tested and compared with the standard model by Cabezón et al. [8]. Prospathopoulos et al. [10] proposed a modification of the k–ω model adjusting the turbulence model coefficients according to lower turbulence decay. Furthermore, the realizability constraint was applied to the k–ω model and its results were compared to the standard model in Ref. [10].

A consistent comparison of the influence of the different turbulence models on the wind turbine simulations is, however, missing. In fact, the k–ε and k–ω formulations followed independent paths with regard to both model tuning and experimental validation. For example, the turbulence constants of the k–ε and k–ω models for atmospheric surface layer and wake simulations were determined by Crespo et al. [4] and Prospathopoulos et al. [9], respectively, with no formal consistency between each other. The same can also be said for the RSM, where no such study was conducted.

This work aims to compare in a consistent way the principal turbulence models present in literature, namely the k–ε, k–ω, and Reynolds stress model, to introduce the SST k–ω model as an innovative turbulence model for wind turbine simulations, and to investigate and assess the influence of the different turbulence models on the results of the CFD simulations. The comparison is made consistent by a proper adjustment of the turbulence model constants according to appropriate experimental observations of atmospheric surface layer and wake flows. The assessment of the turbulence models is conducted by comparing the CFD results with the publicly available experimental measurements of the velocity field and turbulence quantities from two stand-alone wind turbines in the Sexbierum and Nibe wind farms, respectively. Modifications of the derived turbulence model constants are also investigated in order to improve agreement with experimental data.

2 Computational Fluid Dynamics Methodology

The simulation model is based on the RANS equations for incompressible, steady flows, which require additional turbulence modeling to solve the nonlinear Reynolds stress term and to close the system of equations. The set of equations is then composed of the continuity equation

$$\frac{\partial U_i}{\partial x_i} = 0 \tag{1}$$

and the three momentum equations

$$U_j \frac{\partial U_i}{\partial x_j} = -\frac{1}{\rho}\frac{\partial p}{\partial x_i} + \frac{\partial}{\partial x_j}\left[\nu\left(\frac{\partial U_i}{\partial x_j} + \frac{\partial U_j}{\partial x_i}\right) - \overline{u_i u_j}\right] + \frac{f}{\rho} \tag{2}$$

where $U_{i,j}$ is the mean velocity component, p is the mean pressure, ρ and ν are the fluid density and kinematic viscosity, respectively, f is the source term, and i, j are indexes over the coordinate directions. The Reynolds stress term $\overline{u_i u_j}$ is computed with the transport equations for turbulence, whose number depends on the particular choice of the turbulence model. openFOAM[1] is employed to solve this set of equations, using a control-volume-based technique to transform the governing flow equations into algebraic expressions that can be solved numerically. The discretization of the governing equations is based on the second-order upwind scheme, which is applied for the interpolation of velocities and turbulent quantities. The semi-implicit method for pressure-linked equations algorithms is used to solve simultaneously the set of equations by an iterative scheme.

2.1 Turbulence Modeling. This section provides an overview of the turbulence models employed to close the RANS equations, whose effect on the simulations will be discussed in the results section.

2.1.1 Standard k–ε Model. The standard k–ε turbulence model was first proposed by Jones and Launder [12] and was subsequently revised by Launder and Sharma [13] with the introduction of the currently used empirical constants. It was the first two-equation model used in applied computational fluid dynamics and is still the most widely used in many fields [14]. The model is based on the turbulent-viscosity hypothesis (Boussinesq approximation) that relates the Reynolds stresses to the mean flow according to the following equation:

$$-\overline{u_i u_j} = \nu_t\left(\frac{\partial U_i}{\partial x_j} + \frac{\partial U_j}{\partial x_i}\right) - \frac{2}{3}k\delta_{ij} = 2\nu_t S_{ij} - \frac{2}{3}k\delta_{ij} \tag{3}$$

where k is the turbulence kinetic energy, S_{ij} is the mean strain-rate tensor, and ν_t is the eddy viscosity computed as follows:

$$\nu_t = C_\mu \frac{k^2}{\varepsilon} \tag{4}$$

The turbulence kinetic energy, k, and turbulent dissipation rate, ε, are obtained from two transport equations. The standard values of the model constants present in the k and ε equations were chosen in order to impose certain experimental constraints and are the following: $C_\mu = 0.09$, $C_{1\varepsilon} = 1.44$, $C_{2\varepsilon} = 1.92$, $\sigma_k = 1$, $\sigma_\varepsilon = 1.3$. In spite of its broad range of applicability and accurate results for simple flows, the k–ε model has shown some limitations: it can be quite inaccurate for complex flows, in particular in the presence of large adverse pressure gradients [15]. Also, particular near-wall treatments are usually included since the model showed to not perform well for near-wall regions.

2.1.2 Standard k–ω Model. Different formulations of the k–ω turbulence model were proposed in the past, but the standard model adopted today is the one formulated by Wilcox [16], which has been more extensively tested than any other. The model is based on the Boussinesq approximation, and the main difference with respect to the k–ε model is the use of the specific dissipation rate (also called turbulence frequency), ω, in place of the turbulent dissipation rate, ε. Two transport equations are used to calculate the values of k and ω, whereas the eddy viscosity has the following definition:

$$\nu_t = \frac{k}{\omega} \tag{5}$$

The standard constants in the k and ω transport equations take the following values: $\beta^* = 0.09$, $\beta = 0.075$, $\alpha = 0.556$, $\sigma^* = 0.5$, $\sigma = 0.5$.

A close similarity can be observed between the k–ε and the k–ω models when a transformation is applied to the ω equation by adopting the definition of ω as $\varepsilon/(C_\mu k)$ and by using the following transformed constants [17]:

$$\begin{aligned} T &= 1/\omega \\ C_\mu &= \beta^*, \quad C_{1\varepsilon} = 1 + \alpha \\ C_{2\varepsilon} &= 1 + \beta/\beta^*, \quad \sigma_\varepsilon = 1/\sigma \end{aligned} \tag{6}$$

It can be seen that the values of the transformed constants are similar but not exactly equal to the original k–ε values, mainly

[1] http://www.openfoam.com/

Downloaded from http://asmedigitalcollection.asme.org/solarenergyengineering/article-pdf/140/3/031007/6330434/sol_140_03_031007.pdf by Stanford University user on 16 August 2021

because of the calibration of the constants with different (but consistent) experimental data. This transformation reproduces the standard ε model with an additional term S_ω, which is defined as

$$S_\omega = \frac{2}{T}(\nu + \sigma\nu_t)\left(\frac{|\nabla k|^2}{k} - \frac{\nabla k \cdot \nabla \varepsilon}{\varepsilon}\right) \tag{7}$$

This source term in the dissipation equation distinguishes the k–ε and the k–ω models and acts mainly in the inner region of boundary layers (near walls). This characteristic helps to explain why the k–ω model performs better than the k–ε model for boundary-layer flows, both in its treatment of the viscous near-wall region and in its accounting for the effects of streamwise pressure gradient [14]. Two important limitations have, however, to be highlighted: the first is that the model showed problems when dealing with nonturbulent free-stream boundaries so that particular (nonphysical) boundary conditions are usually required; the second is that it overpredicts the level of shear stress in adverse pressure-gradient boundary layers [15].

2.1.3 Shear-Stress Transport k–ω Model. The SST k–ω turbulence model was formulated by Menter [18] and has been found to be quite effective in predicting many aeronautical flows [17]. The reason for this is that it was designed to yield the best behavior of the k–ε and the k–ω models: it retains the robust and accurate formulation of the Wilcox k–ω model in the near wall region, and takes advantage of the freestream independence of the k–ε model in the outer part of the boundary layer. A blending function takes care of the switch between the two models according to the distance from a wall. The blending function F_1 is designed to be one in the near wall region (leading to a k–ω model) and zero away from the surface (leading to a k–ε model). The constants of the model are also calculated by interpolation of the two original models as follows:

$$\phi = F_1\phi_1 + (1 - F_1)\phi_2 \tag{8}$$

The constants of set 1 are from the k–ω model (except σ_{k1}, which is slightly different): $\beta^* = 0.09$, $\beta_1 = 0.075$, $\gamma_1 = 0.556$, $\sigma_{k1} = 0.85$, $\sigma_{\omega 1} = 0.5$. The constants of set 2 are from the k–ε model, derived through Eq. (6): $\beta^* = 0.09$, $\beta_2 = 0.0828$, $\gamma_2 = 0.44$, $\sigma_{k2} = 1$, $\sigma_{\omega 2} = 0.856$.

The other important improvement introduced by Menter in the SST k–ω model with respect to the parent models is in the shear-stress predictions in adverse pressure-gradient boundary layers. The tendency to overestimate the shear stress is fixed by imposing a bound on the stress-intensity ratio, $|\overline{u_i u_j}|/k$. This ratio is often denoted a_1 and in many flows is approximately equal to 0.3, with lower values in adverse pressure gradients. The bound is introduced with a new definition of the eddy viscosity

$$\nu_t = \frac{a_1 k}{\max(a_1\omega; 2|\Omega_{ij}|F_2)} \tag{9}$$

where Ω_{ij} is the mean flow rotation tensor and F_2 is a function that is one for boundary-layer flows and zero for free-shear layers.

2.1.4 Reynolds Stress Model. In the Reynolds stress models, the individual Reynolds stresses are directly computed and consequently the turbulent-viscosity hypothesis is not needed. Six transport equations take care of each Reynolds stress. There exist different approaches to model the terms in the transport equations that have brought about different RSMs: among the most used are the Launder–Reece–Rodi model by Launder et al. [19] and the Speziale–Sarkar–Gatski model by Speziale et al. [20]. In this work it has been chosen to use the Gibson–Launder model [21] which was developed and calibrated with the purpose to accurately simulate atmospheric boundary layers (ABL). This model, as the other RSMs, has six equations to compute each of the six Reynolds stresses and an equation for the turbulent dissipation rate. The standard coefficients of this model are the following: $C_\mu = 0.09$, $C_{1\varepsilon} = 1.44$, $C_{2\varepsilon} = 1.92$, $\sigma_R = 0.8197$, $\sigma_\varepsilon = 1.3$, $C_1 = 1.8$, $C_2 = 0.6$, $C_1' = 0.5$, $C_2' = 0.3$. The first five coefficients are alike the ones in the k–ε model, whereas the others are used to model different terms in the transport equations of the Reynolds stresses.

The RSM is potentially the most general and physically the most complete, since it calculates each of the Reynolds stresses. For this reason, it has also the potential to accurately predict anisotropic turbulent flows, which is an important advantage compared to the eddy viscosity models limited by the Boussinesq approximation and the assumption of isotropic flows. On the other hand, the RSM requires significantly more computational time and CPU memory compared to the simpler two-equation models.

2.2 Actuator Disk Modeling. The wind turbine has been modeled as an actuator disk whose main feature is to apply a distributed force, defined as axial momentum source, F, over a cylindrical volume, defined by the rotor swept area. The actuator disk model, even though it does not provide a detailed description of the wind turbine geometry, is able to capture adequately the wake effect generated by the wind turbine and to compute its power output, as required for the employment in wind turbine and wind farm simulations [22–24]. From the definition of thrust coefficient, it can be derived that the axial force is a function of the reference wind speed

$$F = \frac{1}{2}\rho\frac{\pi D^2}{4}C_T U_{\text{inf}}^2 \tag{10}$$

where ρ is the air density, D is the rotor diameter, U_{inf} is the upstream wind speed, and C_T is the thrust coefficient, obtained from the thrust coefficient curve of the wind turbine at the specified U_{inf}. The power generated can be computed as the product of the axial force and the average velocity over the actuator disk volume V

$$P = F\overline{U_x} = F\frac{1}{V}\int_V U_x dV \tag{11}$$

2.3 Surface Boundary Layer Modeling. The simulations of wind turbines have to take into account the wind conditions and characteristics usually encountered in real flows, which are referred to as ABL. The starting point is the characterization of the mean wind shear profile. For a homogeneous and stationary flow, the shear profile can be described, according to Panofsky and Dutton [25], as

$$\frac{\partial U_x}{\partial z} = \frac{u_*}{\kappa l} \tag{12}$$

where U is the mean wind speed, z is the height above ground, u_* is the local friction velocity, l is the local length scale, and κ is the von Kármán constant ($\approx$0.4). Within the ABL, the friction velocity is expected to decrease with z, vanishing at the edge of the ABL. The expression to account for this variation is the following:

$$u_* = u_{*0}\left(1 - \frac{z}{z_{\max}}\right)^\alpha \tag{13}$$

where $z_{\max}$ is the height of the ABL and α depends on the state of the boundary layer, ranging from 2/3 to 3/2 [26]. The height of an ABL can extend up to some kilometers, depending on the atmospheric stability [25]. The first 10% of the ABL, which is usually called the surface boundary layer (SBL), can be approximated by a constant friction velocity equal to u_{*0}. Also, in the SBL, the length scale is assumed equal to the height ($l_{\text{SL}} = z$).

Downloaded from http://asmedigitalcollection.asme.org/solarenergyengineering/article-pdf/140/3/031007/6330434/sol_140_03_031007.pdf by Stanford University user on 16 August 2021

The length scale, l, is influenced by the atmospheric stability, which describes the combined effects of mechanical turbulence and heat convection, and the height of the ABL. Three classes of atmospheric stability can be defined: unstable, neutral, and stable conditions. The case studies analyzed in this work will take into account only the surface boundary layer in neutral conditions, which is a reasonable approximation up to a height of at least 100 m [25]. Under these hypotheses, a logarithmic velocity profile can be derived from Eq. (12) by integration

$$U_x = \frac{u_{*0}}{\kappa} \ln\left(\frac{z}{z_0}\right) \tag{14}$$

where z_0 is the surface roughness length. This parameter is solely used for describing the wind speed profile; in fact, it is not a physical length, but rather a length scale representing the roughness of the ground (reference values for different terrain types can be found in Ref. [25]). The friction velocity can be calculated once a reference velocity is known at a specific height

$$u_{*0} = \frac{\kappa U_{x,\text{ref}}}{\ln\left(\frac{z_{\text{ref}}}{z_0}\right)} \tag{15}$$

Introducing the equation for the wind profile into the turbulence models, it can be derived that the turbulence kinetic energy, turbulent dissipation rate, and specific dissipation rate have the following expressions, respectively [9,27]:

$$k = \frac{u_{*0}^2}{\sqrt{C_\mu}}, \quad \varepsilon = \frac{u_{*0}^3}{\kappa z}, \quad \omega = \frac{u_{*0}}{\sqrt{\beta^*}\kappa z} \tag{16}$$

Average values for the Reynolds stresses were extrapolated by Panofsky and Dutton [25] from different experimental data sets. The values of the Reynolds stresses reflect the anisotropic nature of the atmospheric boundary layer, and these are given as a function of the friction velocity: $\overline{u_x u_x} = (2.39u_{*0})^2$, $\overline{u_y u_y} = (1.92u_{*0})^2$, $\overline{u_z u_z} = (1.25u_{*0})^2$, $\overline{u_x u_z} = -u_{*0}^2$, $\overline{u_x u_y} = \overline{u_y u_z} = 0$. From the value of the xx-Reynolds stress, Prospathopoulos et al. [9] derived a useful relation between the surface roughness length and the streamwise turbulence intensity, TI_x, which is a common parameter used to characterize the flow turbulent conditions. Following the definition of turbulence intensity (TI), it is possible to write

$$\text{TI}_x = \frac{\overline{u_x}}{U_{x,\text{ref}}} = 2.39\frac{u_{*0}}{U_{x,\text{ref}}} \tag{17}$$

Introducing Eq. (15) on the right-hand side of Eq. (17), it is possible to rearrange the equation in order to find the value of the surface roughness length as a function of the turbulence intensity

$$z_0 = z_{\text{ref}} \exp\left(\frac{-0.980}{\text{TI}_x}\right) \tag{18}$$

Starting from the definition of turbulence kinetic energy, it is also straightforward to derive a relation between the turbulence kinetic energy and the streamwise turbulence intensity

$$k = \frac{1}{2}(\overline{u_x u_x} + \overline{u_y u_y} + \overline{u_z u_z}) = 5.48u_{*0}^2 = 0.959\text{TI}_x^2 U_{x,\text{ref}}^2 \tag{19}$$

3 Turbulence Model Constants for Surface Boundary Layer and Wind Turbine Simulations

The standard coefficients of the turbulence models previously described have been calibrated on several and various experimental data sets, and therefore represent a compromise to give the best performance for a range of flows [14]. The conditions that a wind turbine simulation has to deal with represent a particular subset of the entire range of the turbulence model applicability. In particular, two main phenomena occurring in this application can be identified: the SBL and the wake generated by the wind turbine that propagates in an SBL. Taking this into account, it is possible to reduce the range of applicability of the turbulence models to the particular flow situations previously mentioned and recalibrate the turbulence model constants with more convenient measurements from SBL and wake flows. Crespo et al. [4] and Prospathopoulos et al. [9] were the first to propose a modification of the constants for the k–ε and the k–ω models, respectively, for wind turbine simulation is SBL flows. A consistent adjustment of the coefficients for the aforementioned turbulence models has not been formulated yet and it is proposed in this study in accordance with previous works and convenient data sets for wind turbine simulations. Furthermore, modifications of the derived turbulence model constants are also investigated in order to improve agreement with experimental data considering different values of turbulence decay. In total, three sets of coefficients (one baseline and two modifications) are determined and tested on wind turbine simulations.

The first coefficient analyzed is C_μ, equivalent to β^*, which appears in the definition of the turbulent viscosity (Eq. (4)). The standard value was determined according to measurements from simple turbulent shear flows and the logarithmic region of boundary layers; in these particular situations, it is possible to demonstrate that [14]

$$C_\mu = \left(\frac{|\overline{u_i u_j}|}{k}\right)^2 \tag{20}$$

The stress-intensity ratio was measured to be approximately 0.3 in those flows and C_μ was calculated accordingly, giving the standard value of 0.09. When dealing with SBL, the stress-intensity ratio assumes, as shown in Sec. 2.3, the following value:

$$\frac{|\overline{u_i u_j}|}{k} = \frac{u_{*0}^2}{k} = 0.182 \tag{21}$$

Therefore, the value of C_μ is changed in this work to 0.0333, as also reported in Refs. [4] and [9]. On the other hand, there are no specific measurements from wind turbine wake flows that can support the validity of this coefficient also in wind turbine wake simulations. Nevertheless, the value of the stress-intensity ratio is supposed to be valid also in the wake of wind turbines operating in SBL flows, based on the consideration that turbulence "remembers" the upstream conditions much longer than the average wind speed. In particular, the anisotropy present in the SBL is expected to be retained at some level also in wind turbine wakes, implying that the proposed value can be a good approximation for both cases. Beside this consideration, Durbin and Petterson [17], in a more general discussion on the applicability of the turbulence models, suggested that the value of C_μ should be adjusted based on more recent experimental data, proposing a value close to the one introduced for SBL and wake flows.

The second coefficient analyzed is $C_{2\varepsilon}$ (equivalent to $\beta = (C_{2\varepsilon} - 1)\beta^*$), which controls the decaying of turbulence. It is possible to show that in the particular case of homogeneous, isotropic turbulence, the decaying of turbulence is controlled by a power-law solution [14]. The decay exponent, n, characterizing the solution is correlated to the $C_{2\varepsilon}$ coefficient according to the following relation:

$$C_{2\varepsilon} = \frac{n+1}{n} \tag{22}$$

Measurements of grid turbulence in wind tunnels give a value for n in the range of 1.3 ± 0.2 [17]. The standard values of the k–ε

Downloaded from http://asmedigitalcollection.asme.org/solarenergyengineering/article-pdf/140/3/031007/6330434/sol_140_03_031007.pdf by Stanford University user on 16 August 2021

Table 1 Baseline turbulence model constants derived for a turbulence decay exponent of 1.2

Turbulence model	Turbulence constants				
k–ε	$C_\mu = 0.0333$	$C_{1\varepsilon} = 1.42$	$C_{2\varepsilon} = 1.83$	$\sigma_k = 2.25$	$\sigma_\varepsilon = 2.25$
k–ω	$\beta^* = 0.0333$	$\alpha = 0.42$	$\beta = 0.0277$	$\sigma^* = 0.45$	$\sigma = 0.45$
SST k–ω	$\beta^* = 0.0333$	$\gamma_1 = 0.42$ $\gamma_2 = 0.42$	$\beta_1 = 0.0277$ $\beta_2 = 0.0277$	$\sigma_{k1} = 0.45$ $\sigma_{k2} = 0.45$	$\sigma_{\omega1} = 0.45$ $\sigma_{\omega2} = 0.45$
RSM	$C_\mu = 0.0333$	$C_{1\varepsilon} = 1.42$ $C_1 = 1.8$	$C_{2\varepsilon} = 1.83$ $C_2 = 0.6$	$\sigma_R = 0.8197$ $C_1^{'} = 0.5$	$\sigma_\varepsilon = 2.25$ $C_2^{'} = 0.3$

Table 2 Modified turbulence model constants derived for a turbulence decay exponent of 0.9

Turbulence model	Turbulence constants				
k–ε	$C_\mu = 0.0333$	$C_{1\varepsilon} = 1.65$	$C_{2\varepsilon} = 2.11$	$\sigma_k = 2.0$	$\sigma_\varepsilon = 2.0$
k–ω	$\beta^* = 0.0333$	$\alpha = 0.65$	$\beta = 0.0367$	$\sigma^* = 0.5$	$\sigma = 0.5$
SST k–ω	$\beta^* = 0.0333$	$\gamma_1 = 0.65$ $\gamma_2 = 0.65$	$\beta_1 = 0.0367$ $\beta_2 = 0.0367$	$\sigma_{k1} = 0.5$ $\sigma_{k2} = 0.5$	$\sigma_{\omega1} = 0.5$ $\sigma_{\omega2} = 0.5$
RSM	$C_\mu = 0.0333$	$C_{1\varepsilon} = 1.65$ $C_1 = 1.8$	$C_{2\varepsilon} = 2.11$ $C_2 = 0.6$	$\sigma_R = 0.8197$ $C_1^{'} = 0.5$	$\sigma_\varepsilon = 2.0$ $C_2^{'} = 0.3$

Table 3 Modified turbulence model constants derived for a turbulence decay exponent of 0.6

Turbulence model	Turbulence constants				
k–ε	$C_\mu = 0.0333$	$C_{1\varepsilon} = 2.16$	$C_{2\varepsilon} = 2.67$	$\sigma_k = 1.84$	$\sigma_\varepsilon = 1.84$
k–ω	$\beta^* = 0.0333$	$\alpha = 1.16$	$\beta = 0.055$	$\sigma^* = 0.54$	$\sigma = 0.54$
SST k–ω	$\beta^* = 0.0333$	$\gamma_1 = 1.16$ $\gamma_2 = 1.16$	$\beta_1 = 0.055$ $\beta_2 = 0.055$	$\sigma_{k1} = 0.54$ $\sigma_{k2} = 0.54$	$\sigma_{\omega1} = 0.54$ $\sigma_{\omega2} = 0.54$
RSM	$C_\mu = 0.0333$	$C_{1\varepsilon} = 2.16$ $C_1 = 1.8$	$C_{2\varepsilon} = 2.67$ $C_2 = 0.6$	$\sigma_R = 0.8197$ $C_1^{'} = 0.5$	$\sigma_\varepsilon = 1.84$ $C_2^{'} = 0.3$

and k–ω models are 1.09 and 1.2, respectively. The turbulence decay is expected to behave in a similar manner also in the SBL and wake flows, and therefore the value of the decay exponent can be considered to fall in the same range. However, Prospathopoulos et al. [10] suggested that the exponent could be lower for the anisotropic SBL flow. They tested that assumption on a standard k–ω model, providing some improvements to the simulation predictions. Following their approach, three values were chosen in this work: 1.2 (the baseline one), 0.9, and 0.6 (the two modifications). The turbulence model constants were computed accordingly in order to guarantee consistency.

The coefficient $C_{1\varepsilon}$ (equivalent to $\alpha = C_{1\varepsilon} - 1$), for given values of C_μ and $C_{2\varepsilon}$, controls the spreading rate of free-shear flows [17]. The standard value was chosen so that the basic model would give a reasonable value for the spreading rate in mixing layers. What actually determines the spreading rate of free-shear flows in numerical simulations is the difference $C_{2\varepsilon} - C_{1\varepsilon}$: a difference of about $0.45 - 0.50$ gives a good estimation of this quantity and this is how the standard coefficients were determined [17]. Mixing layers are an occurring phenomenon in the wakes of wind turbine and the constraint previously mentioned has to be taken into account. This was not the case when the modifications of the standard coefficients were first proposed in Refs. [4] and [9] for SBL, and a different modification is proposed here on the basis of the aforementioned constraint. Given the values of C_μ and $C_{2\varepsilon}$ previously determined, values of $C_{1\varepsilon}$ are determined according to the difference $C_{2\varepsilon} - C_{1\varepsilon}$.

The value of the coefficient σ_ε (equivalent to $1/\sigma$) can be established by examining the log region in boundary layers. Under this condition, the following equation must hold [14]:

$$\kappa^2 = \sigma_\varepsilon \sqrt{C_\mu}(C_{2\varepsilon} - C_{1\varepsilon}) \tag{23}$$

from which it is possible to calculate the value for σ_ε, given the other coefficients already determined and the value of the von Kármán constant.

The last coefficient that has to be discussed is σ_k (equivalent to $1/\sigma^*$). Differently from the other coefficients, there are no particular cases with whom its value can be determined. In fact, for the standard k–ε model, its value is set to 1, whereas for the k–ω model, its value is kept equal to σ, as a tradeoff among a broad range of experimental observations [15]. This second approach has been chosen in this work.

The final sets of coefficients for each turbulence model are summarized in Tables 1–3 for the baseline and modifications, respectively.

4 Case Studies

The validation of the CFD model with the aforementioned turbulence closures and SBL equations was conducted using the experimental data sets from the Sexbierum [28] and Nibe [29] wind farms.

4.1 Sexbierum Wind Farm. The Dutch Experimental Wind Farm at Sexbierum is located in the Northern part of The Netherlands at approximately 4 km distance of the seashore. The wind farm is located in flat homogeneous terrain, mainly grassland used by farmers. The wind farm has a total of 5.4 MW installed capacity consisting of 18 turbines of 300 kW rated power each.

Downloaded from http://asmedigitalcollection.asme.org/solarenergyengineering/article-pdf/140/3/031007/6330434/sol_140_03_031007.pdf by Stanford University user on 16 August 2021

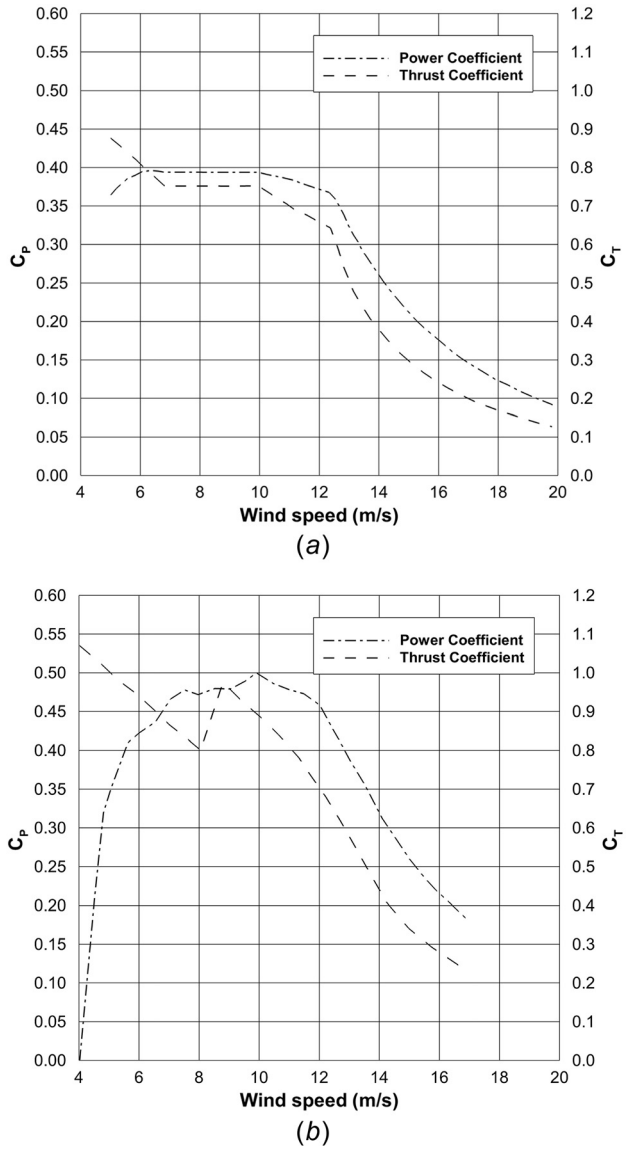

Fig. 1 Performance curves of the Sexbierum and Nibe wind turbines: (*a*) Sexbierum wind turbine and (*b*) Nibe wind turbine

The wind turbines in the wind farm are HOLEC machines with three WPS 30/3 blades, a rotor diameter of 30.1 m, and a hub height of 35 m. Performance curves are reported in Fig. 1(*a*). The campaign concerned measurement of the wind speed, turbulence and shear stress behind a single wind turbine at distances of 2.5, 5.5 and 8 rotor diameters, respectively. The free stream wind conditions at hub height were $U_{\text{inf}} = 10$ m/s and $\text{TI}_x = 10\%$. For these conditions, the thrust coefficient was $C_T = 0.75$.

4.2 Nibe Wind Farm. The Nibe wind farm is located on a coastal site near Aalborg in the norther Jutland, Denmark. It is constituted by two machines (A and B) located 200 m apart from each other along an approximately North-South axis, which runs parallel to the coast line. To the west, there is a fetch of at least 6 km over open, shallow water. On the landward site, the ground surrounding the site is flat, grass-covered, and free of significant obstacles. The two wind turbines are almost identical, both with a rated power of 630 kW. The rotor diameter is 40 m, the hub height is 45 m. Performance curves are reported in Fig. 1(*b*). The data examined here correspond to the turbine B operating alone, and measurements of wind speed and turbulence are available behind the turbine at distances of 2.5, 4 and 7.5 rotor diameters, respectively. The free stream wind conditions at hub height were $U_{\text{inf}} = 8.5$ m/s and $\text{TI}_x = 10\%$. For these conditions, the thrust coefficient was estimated to be $C_T = 0.82$.

Table 4 Wind turbine characteristics and wind conditions of Sexbierum and Nibe wind farms

Wind turbine	D (m)	H (m)	U_{inf} (m/s)	TI_x (%)	C_T
Sexbierum	30.1	35	10	10	0.75
Nibe	40	45	8.5	10	0.82

Table 4 summarizes the wind turbine characteristics and wind conditions.

5 Numerical Setup

The computational domain and mesh of the two cases were generated with *blockMesh* and *snappyHexMesh*, two mesh utilities of OpenFOAM for mesh generation and refinement, respectively. The Cartesian coordinate system is defined with x, y, and z being respectively the streamwise, lateral and vertical directions. Figure 2 illustrates schematic layouts of the domain. The dimensions of the domain are a function of the rotor diameter. The domain includes the actuator disk region and a refined region surrounding the disk with a double mesh resolution in order to capture the most significant gradients in the flow field.

The dimensions of the domain were carefully determined in order not to influence the flow-field solution and to avoid useless

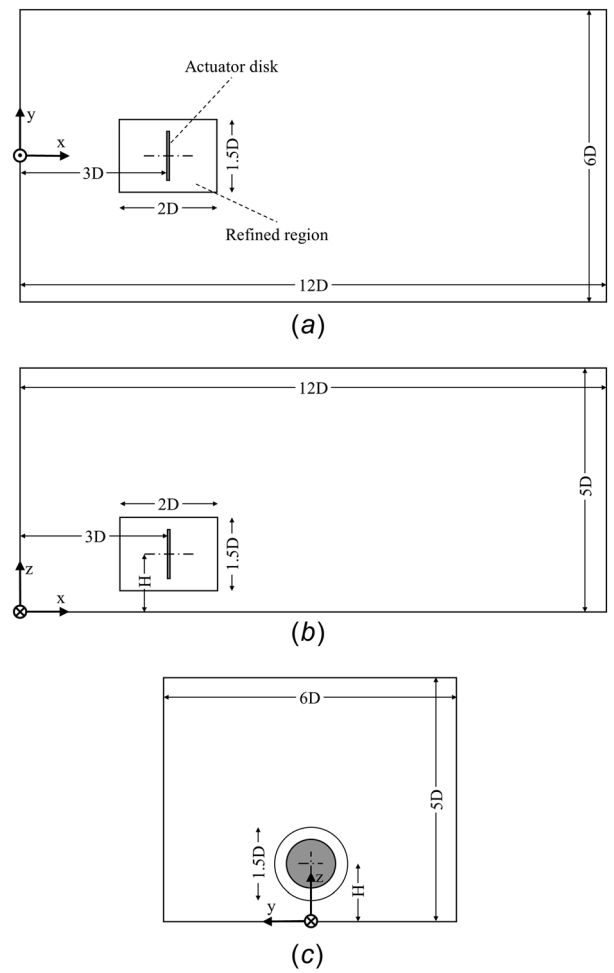

Fig. 2 Schematic layouts of the domain: (*a*) top view, (*b*) lateral view, and (*c*) front view

Downloaded from http://asmedigitalcollection.asme.org/solarenergyengineering/article-pdf/140/3/031007/6330434/sol_140_03_031007.pdf by Stanford University user on 16 August 2021

Table 5 RMSE between the experimental data and the simulations results when considering the wind direction range between −30 deg and 30 deg. The RMSEs are classified by case (Sexbierum and Nibe), by quantity of interest (normalized wind speed (NWS), normalized turbulence kinetic energy (NTKE), and TI), by downstream distance, and by turbulence model.

			k–ε			k–ω		
Wind turbine	Quantity	Distance	baseline	1	2	baseline	1	2
Sexbierum	NWS	2.5D	0.1859	0.1691	0.1328	0.1936	0.1796	0.1480
		5.5D	0.0730	0.0656	0.0502	0.0804	0.0747	0.0610
		8D	0.0545	0.0510	0.0449	0.0603	0.0577	0.0518
	NTKE	2.5D	0.0114	0.0116	0.0121	0.0114	0.0115	0.0118
		5.5D	0.0044	0.0046	0.0050	0.0044	0.0045	0.0048
		8D	0.0042	0.0042	0.0038	0.0042	0.0041	0.0040
Nibe	NWS	2.5D	0.1848	0.1625	0.1119	0.1936	0.1757	0.1324
		4D	0.0683	0.0560	0.0386	0.0738	0.0641	0.0428
		7.5D	0.0453	0.0425	0.0424	0.0468	0.0439	0.0394
	TI	2.5D	0.0300	0.0282	0.0190	0.0301	0.0290	0.0223
		4D	0.0239	0.0233	0.0182	0.0236	0.0235	0.0206
		7.5D	0.0217	0.0210	0.0180	0.0215	0.0212	0.0195
				SST k–ω			RSM	
Wind turbine	Quantity	Distance	baseline	1	2	baseline	1	2
Sexbierum	NWS	2.5D	0.0947	0.0916	0.0878	0.0797	0.0794	0.0789
		5.5D	0.0468	0.0512	0.0601	0.0462	0.0436	0.0427
		8D	0.0480	0.0514	0.0584	0.0431	0.0419	0.0425
	NTKE	2.5D	0.0148	0.0155	0.0169	0.0149	0.0147	0.0145
		5.5D	0.0057	0.0063	0.0073	0.0045	0.0047	0.0053
		8D	0.0038	0.0037	0.0040	0.0036	0.0035	0.0034
Nibe	NWS	2.5D	0.0614	0.0568	0.0531	0.0510	0.0496	0.0475
		4D	0.0619	0.0752	0.0912	0.0776	0.0730	0.0705
		7.5D	0.0505	0.0595	0.0723	0.0435	0.0417	0.0440
	TI	2.5D	0.0202	0.0241	0.0313	0.0147	0.0141	0.0137
		4D	0.0149	0.0157	0.0207	0.0182	0.0176	0.0129
		7.5D	0.0163	0.0147	0.0146	0.0208	0.0178	0.0137

domain regions. In particular, larger dimensions were tested and were subsequently decreased according to the following rule: a smaller domain is accepted only if the flow solution does not vary by more than 1% with respect to the largest domain tested (with dimensions as double as the ones presented here), ideally considered as the solution of an infinite domain. The dimensions that need a detailed discussion are the distance between the inlet and the wind turbine, and the height of the domain. In the first case, there has to be enough distance before the wind turbine to allow the flow field perturbed by the wind turbine to propagate upstream without being influences by the inlet boundary conditions. A distance of 3D was found to correctly satisfy this condition. In the second case, a too short domain height would cause flow blockage and would promote a faster, nonphysical wake recovery. A height of 5D was determined according to these considerations and to practical wind engineering reference guideline, which suggests a value of 5H, being H the height of any obstacle (in this case the wind turbine rotor). The other dimensions were basically chosen in order to have the flow-field solution as far as the experimental measurements are available for comparison.

For the solution of the RANS equations, the convergence criterion was set so that the residuals of all the equations were below 10^{-5}. A stricter convergence criterion was found to provide a negligible difference on the solution.

5.1 Boundary Conditions. The inlet boundary condition was defined with the equations relative to the SBL. Given the flow characteristics, i.e., U_{inf}, TI_x, and H, the values for z_0 and u_{*0} were derived with Eqs. (15) and (18). The velocity, turbulence kinetic energy (or Reynolds stresses), and turbulence dissipation rate (or specific dissipation rate) were then prescribed according to Eqs. (14) and (16), depending on the turbulence model used. The outlet boundary condition was defined as a pressure outlet, with zero gradient for the velocity and turbulence quantities. The top boundary condition was defined by prescribing constant values of velocity, turbulence kinetic energy (or Reynolds stresses), and turbulence dissipation rate (or specific dissipation rate) at the domain height, whereas zero gradient was set for the pressure. The side boundary condition was defined as zero gradient for all the variables. The ground was defined as a rough wall, with wall functions that took care of the turbulence quantities.

5.2 Wall Functions. A proper treatment of the ground surface is essential to correctly simulate SBL flows. A general requirement of CFD simulations consists in having a very fine mesh in proximity of any surface in order to capture the large velocity gradients and to compute a correct wall shear stress. In SBL simulations, this is impossible because the surface roughness prevents a full solution of the boundary layers. In fact, the first wall-adjacent cell should be at least the double of the surface roughness, which is in conflict with the requirement of a high mesh resolution. In these cases, wall functions based on log-law boundary layers for rough walls are used to calculate the turbulent viscosity and wall shear stress. Blocken et al. [30] discussed the problem of the wall treatment for these particular flows, suggesting remedies when the simulations are run with ANSYS FLUENT or CFX (which adopt wall functions based on an equivalent sand-grain roughness, k_S, equivalent to approximately $30z_0$). OPENFOAM, differently from the previously mentioned CFD packages, has a wall function which is based on the actual surface roughness length, z_0, and which is derived from Eq. (14). This was used in the present work and allowed to have a higher resolution close to the wall than the one reached with ANSYS FLUENT and CFX.

Downloaded from http://asmedigitalcollection.asme.org/solarenergyengineering/article-pdf/140/3/031007/6330434/sol_140_03_031007.pdf by Stanford University user on 16 August 2021

A value of approximately 0.01D for the first cell at the wall was found to guarantee a correct simulation of SBL flows, achieving horizontally homogeneity (i.e., zero streamwise gradients) of the SBL in an empty domain. This value is also consistent with other works present in literature [8,10].

5.3 Mesh Sensitivity Analysis. A mesh sensitivity analysis was conducted in order to reduce spatial discretization errors in the CFD simulations and to guarantee a mesh-independent solution. Different grid resolutions were tested for each turbulence model and the relative error of the designated flow variables was measured. The global grid spacing was decreased progressively by a factor of 1.5, starting from the coarsest case where the global spacing was 0.225D. The resolution in the refined region surrounding the wind turbine was as double as the global resolution. In the region close to the wall, the resolution was also higher: the first cell at the wall was fixed to a height of 0.01D and this value was progressively increased moving away from the wall, up to the size given by the global resolution. The height of the region where this mesh refinement took place was 0.5D.

Given the aforementioned considerations, four different global grid spacings were tested, namely 0.225D, 0.150D, 0.100D, and 0.067D, and the value of streamwise velocity was monitored at two locations downstream the wind turbine, namely 2.5D and 8D for the Sexbierum case, and 2.5D and 7.5D for the Nibe case. The number of cells obtained for the different resolutions was approximately 40·, 130·, 400·, and 1300×10^3, respectively. A global grid spacing of 0.1D was found to guarantee a mesh independent solution: the percentage difference of the calculated velocities and turbulence quantities for all the turbulence models with respect to a lower grid spacing (0.067D) was found to be less than 1%. This result is consistent with other computational studies on wind turbine wake simulations [8,10,31].

6 Results and Discussion

This section includes the results obtained from the developed CFD wake model when applied to the stand-alone Sexbierum and Nibe wind turbine cases. The simulated wind speed and turbulent quantities were compared with the real wind turbine measurements in order to assess the implemented turbulence models and the CFD model as a whole. Root-mean-square errors (RMSE) were calculated between the experimental data and the simulations results and are reported in Table 5. The simulations were solved with *simpleFoam*, the OpenFOAM steady-state solver for incompressible, turbulent flows, that run on a Inter(R) Core(TM) i7-4790 computer with 3.60 Ghz clock time using six processors. The number of iterations required to reach the convergence of the solution was about 400 for the k–ε and k–ω models, 300 for the SST k–ω model, and 800 for the RSM. The computational time required for the simulations to converge ranged from approximately 20 min for the SST k–ω model to 40 min for the RSM.

Figures 3–6 show the normalized wind speed and the turbulence kinetic energy downstream the Sexbierum wind turbine as a function of the wind direction. The comparison with experimental data was conducted at three downstream locations, namely 2.5D, 5.5D, and 8D downstream the wind turbine, in order to assess the numerical results obtained with the four turbulence models. The wind direction refers to relative direction of the incoming flow where 0deg indicates the direction behind the center of the rotor at which the maximum wind speed deficit is expected.

With regard to the results for the baseline coefficients, the wind speed was captured well by the SST k–ω and Reynolds stress models for the three locations, but it was highly overestimated by the k–ε and k–ω models, especially at 2.5D downstream where the RMSEs were the highest (0.1859 and 0.1936, respectively). This overestimation is consistent with previous works that highlighted the limitations of these two models [7,10]. The reason of the

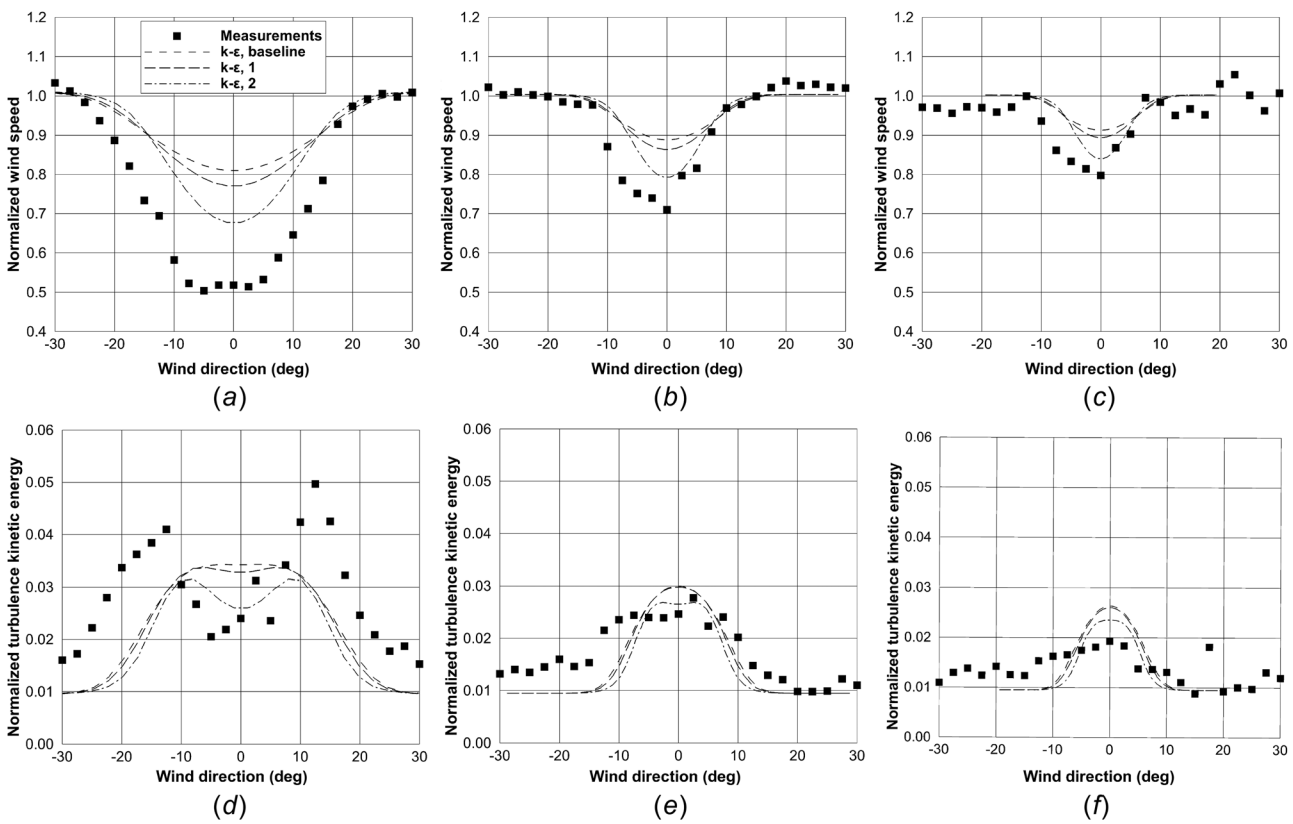

Fig. 3 Wind speed and turbulence kinetic energy downstream the Sexbierum wind turbine as a function of wind direction for the k–ϵ model with the baseline and modified sets of coefficients: (*a*) 2.5D downstream, (*b*) 5.5D downstream, (*c*) 8D downstream, (*d*) 2.5D downstream, (*e*) 5.5D downstream, and (*f*) 8D downstream

Downloaded from http://asmedigitalcollection.asme.org/solarenergyengineering/article-pdf/140/3/031007/6330434/sol_140_03_031007.pdf by Stanford University user on 16 August 2021

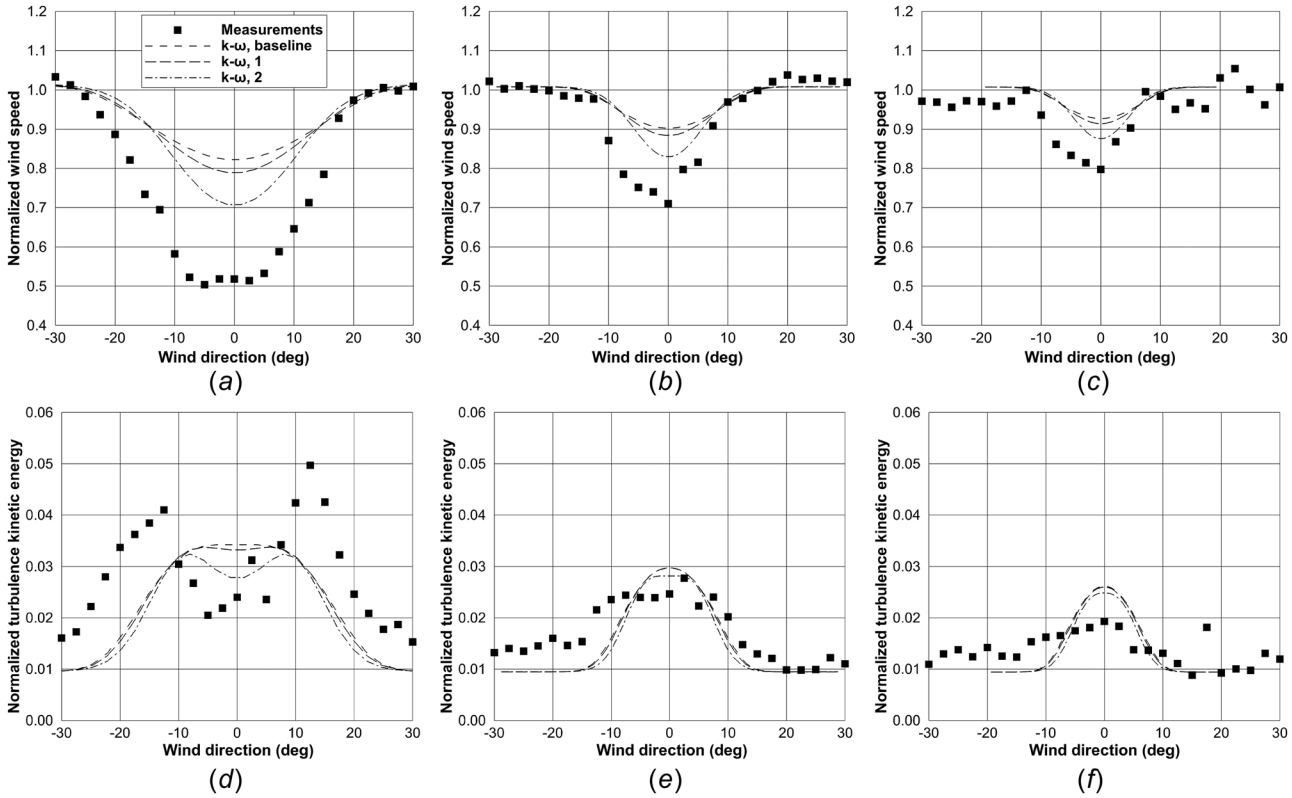

Fig. 4 Wind speed and turbulence kinetic energy downstream the Sexbierum wind turbine as a function of wind direction for the *k–ω* model with the baseline and modified sets of coefficients: (*a*) 2.5*D* downstream, (*b*) 5.5*D* downstream, (*c*) 8*D* downstream, (*d*) 2.5*D* downstream, (*e*) 5.5*D* downstream, and (*f*) 8*D* downstream

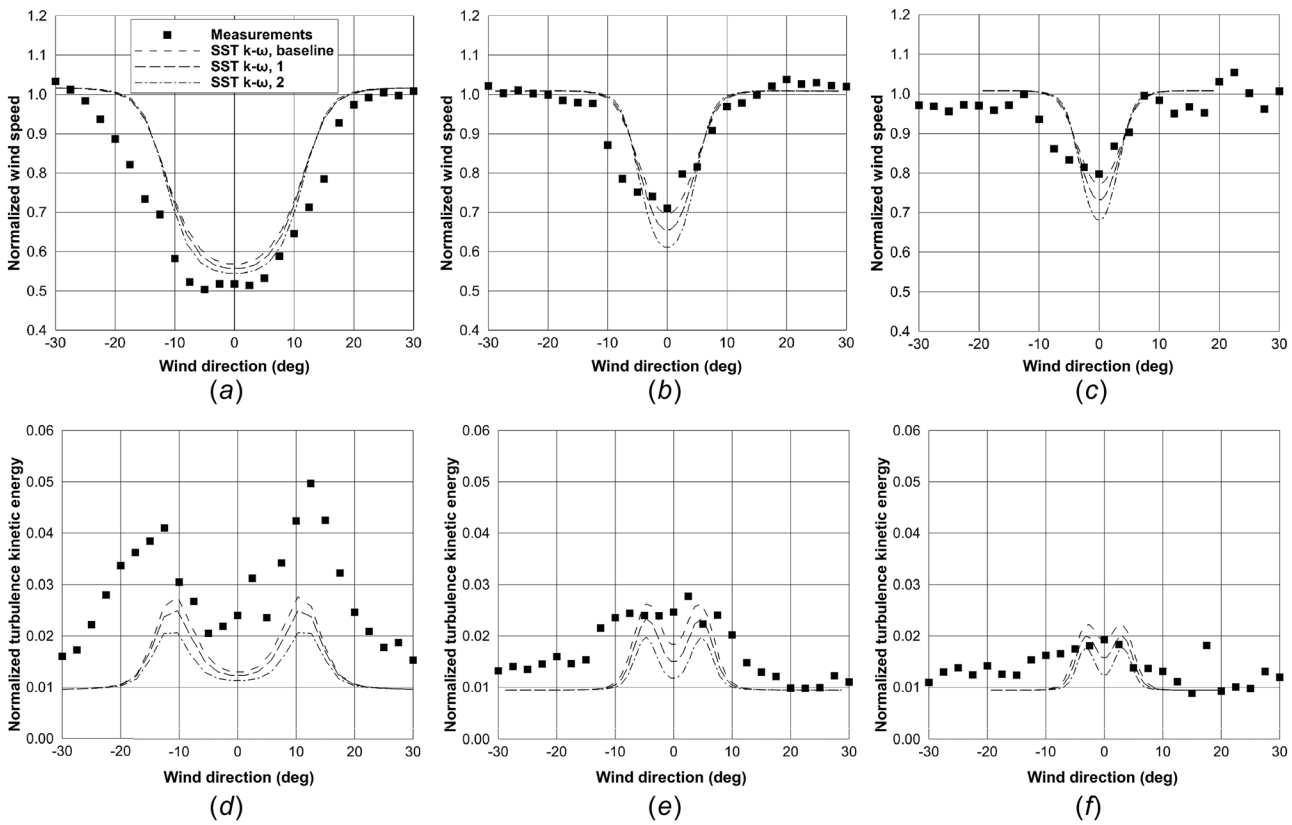

Fig. 5 Wind speed and turbulence kinetic energy downstream the Sexbierum wind turbine as a function of wind direction for the *SST k–ω* model with the baseline and modified sets of coefficients: (*a*) 2.5*D* downstream, (*b*) 5.5*D* downstream, (*c*) 8*D* downstream, (*d*) 2.5*D* downstream, (*e*) 5.5*D* downstream, and (*f*) 8*D* downstream

Downloaded from http://asmedigitalcollection.asme.org/solarenergyengineering/article-pdf/140/3/031007/6330434/sol_140_03_031007.pdf by Stanford University user on 16 August 2021

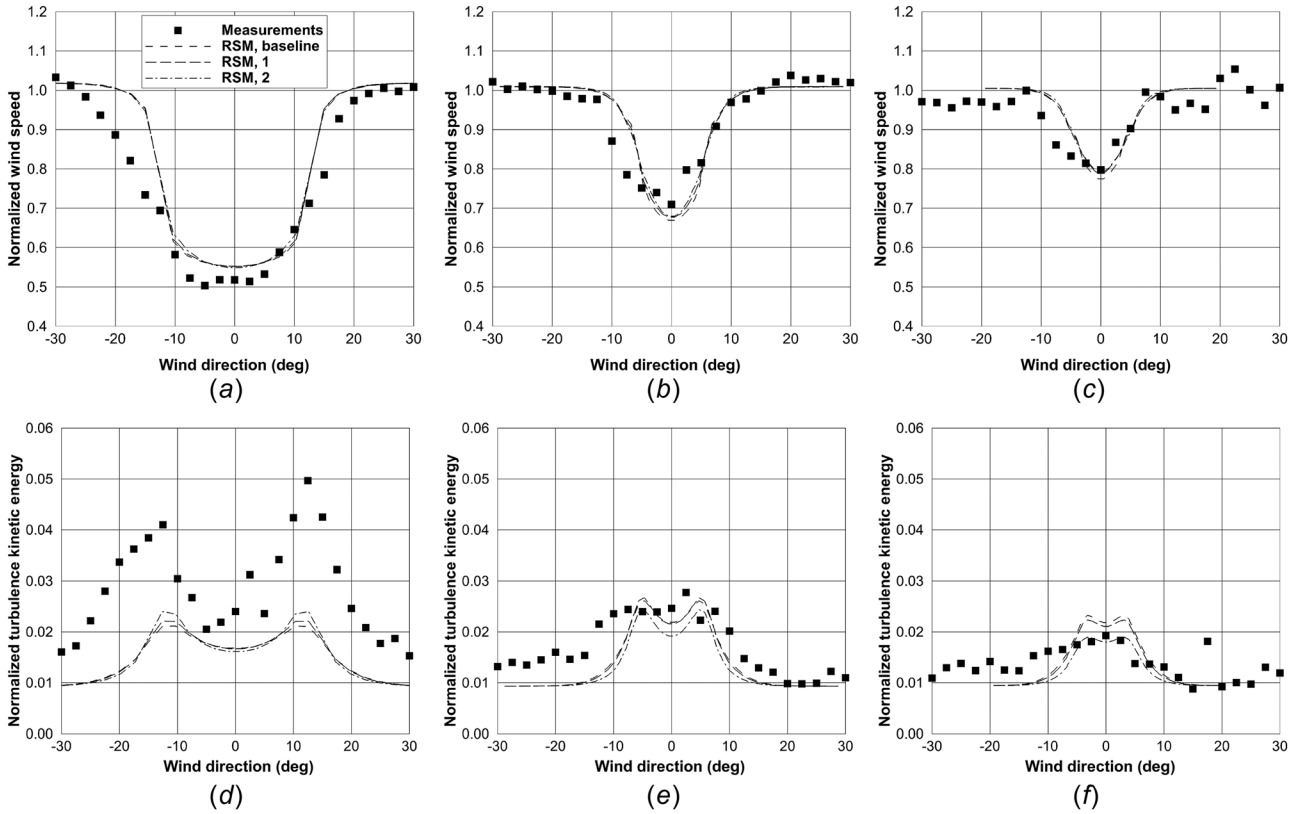

Fig. 6 Wind speed and turbulence kinetic energy downstream the Sexbierum wind turbine as a function of wind direction for the RSM with the baseline and modified sets of coefficients: (*a*) 2.5*D* downstream, (*b*) 5.5*D* downstream, (*c*) 8*D* downstream, (*d*) 2.5*D* downstream, (*e*) 5.5*D* downstream, and (*f*) 8*D* downstream

failure is very likely caused by the incorrect prediction of the eddy viscosity in situations of adverse pressure gradients, such as the one experienced in the near wake of the wind turbine. Indeed, the results with the SST k–ω model, whose eddy viscosity is bounded to prevent the aforementioned behavior, were accurate and very similar to the predictions of the RSM, which does not rely on the turbulent-viscosity hypothesis.

Similar results can be observed for the turbulence kinetic energy in the Sexbierum case. The k–ε and k–ω models were unable to predict the peaks of turbulence kinetic energy generated by the tip vortexes which are present in the near wake of a wind turbine. Further downstream, the turbulence kinetic energy profile was more homogeneous and the predictions of the two models were improved. The SST k–ω and Reynolds stress models provided a turbulence kinetic energy profile which was similar to the experimental data but the predicted value was slightly underestimated. Also in this case, their predictions improved in the far wake providing a good agreement with the experimental data.

Figures 7–10 show the normalized wind speed and the turbulence intensity downstream the Nibe wind turbine as a function of the wind direction. The streamwise turbulence intensity could not be computed directly from the eddy-viscosity CFD simulations (k–ε, k–ω and SST k–ω), but was instead obtained with the inverse of Eq. (19) assuming that the anisotropy present in the SBL is retained also in the wind turbine wake. Similarly to the previous case, the comparison with experimental data was conducted at three downstream locations, namely 2.5D, 4D, and 7.5D downstream the wind turbine.

The prediction of wind speed in the Nibe case by the baseline turbulence models presented similar characteristics to the previous case. At the location 2.5D downstream the wind turbine the results provided by the SST k–ω and Reynolds stress models matched very well the experimental observations (RMSEs of 0.0614 and 0.0510, respectively), whereas the agreement was not as good for the locations further downstream where an underestimation of the wind speed was observed. This underestimation of the far-wake velocity is likely caused by unsteady phenomena (meandering of the wake) that were not taken into account in the simulations. The k–ε and k–ω models, instead, provided a wind speed significantly higher than the observed (the highest RMSEs were 0.1848 and 0.1936, respectively).

Focusing on the turbulence intensity provided by the baseline turbulence models, it is possible to see that the k–ε and k–ω models exhibited the same incorrect behavior as previously discussed. The predicted turbulence intensity profile did not show the characteristic peaks in the near wake of the wind turbine, and the predicted values were also generally higher that the experimental data for all the three locations. A much better agreement was observed using the SST k–ω and Reynolds stress models, both in terms of intensity and profile. The similar values of turbulence intensity obtained by the SST k–ω and Reynolds stress models supports the assumption made to calculate it. A remark has to be made on the low level of turbulence intensity observed experimentally for wind directions higher than 20deg (right side of the figures): winds coming from those directions experience open, shallow water and are characterized by lower turbulence intensity, which was not taken into account in the simulations.

The modified sets of turbulence constants, determined following the proposition of Prospathopoulos et al. [10], had the effect of decreasing the wind speed and the wind speed recovery. This is particularly evident for the k–ε and k–ω models, whose predictions are improved with respect to the baseline set of coefficients in the two cases analyzed. The highest RMSEs decreased to 0.1328 and 0.1480 for the Sexbierum case and to 0.1119 and 0.1324 for the Nibe case, respectively. The improvement was even more evident for the other locations. This trend suggests that decreasing the decay exponent is beneficial for the k–ε and k–ω models. On the other hand, the effect of decreasing the decay

Downloaded from http://asmedigitalcollection.asme.org/solarenergyengineering/article-pdf/140/3/031007/6330434/sol_140_03_031007.pdf by Stanford University user on 16 August 2021

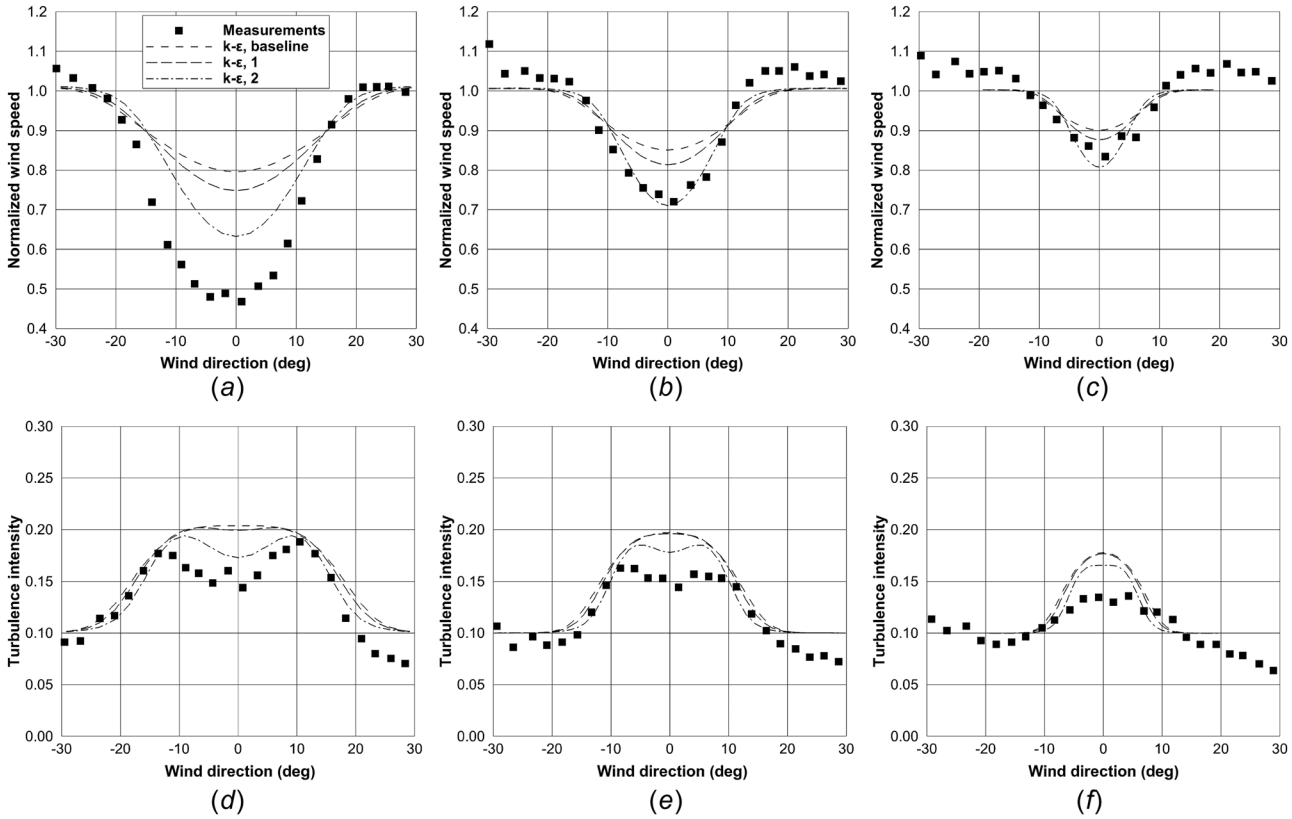

Fig. 7 Wind speed and TI downstream the Nibe wind turbine as a function of wind direction for the k–ϵ model with the baseline and modified sets of coefficients: (*a*) 2.5*D* downstream, (*b*) 4*D* downstream, (*c*) 7.5*D* downstream, (*d*) 2.5*D* downstream, (*e*) 4*D* downstream, and (*f*) 7.5*D* downstream

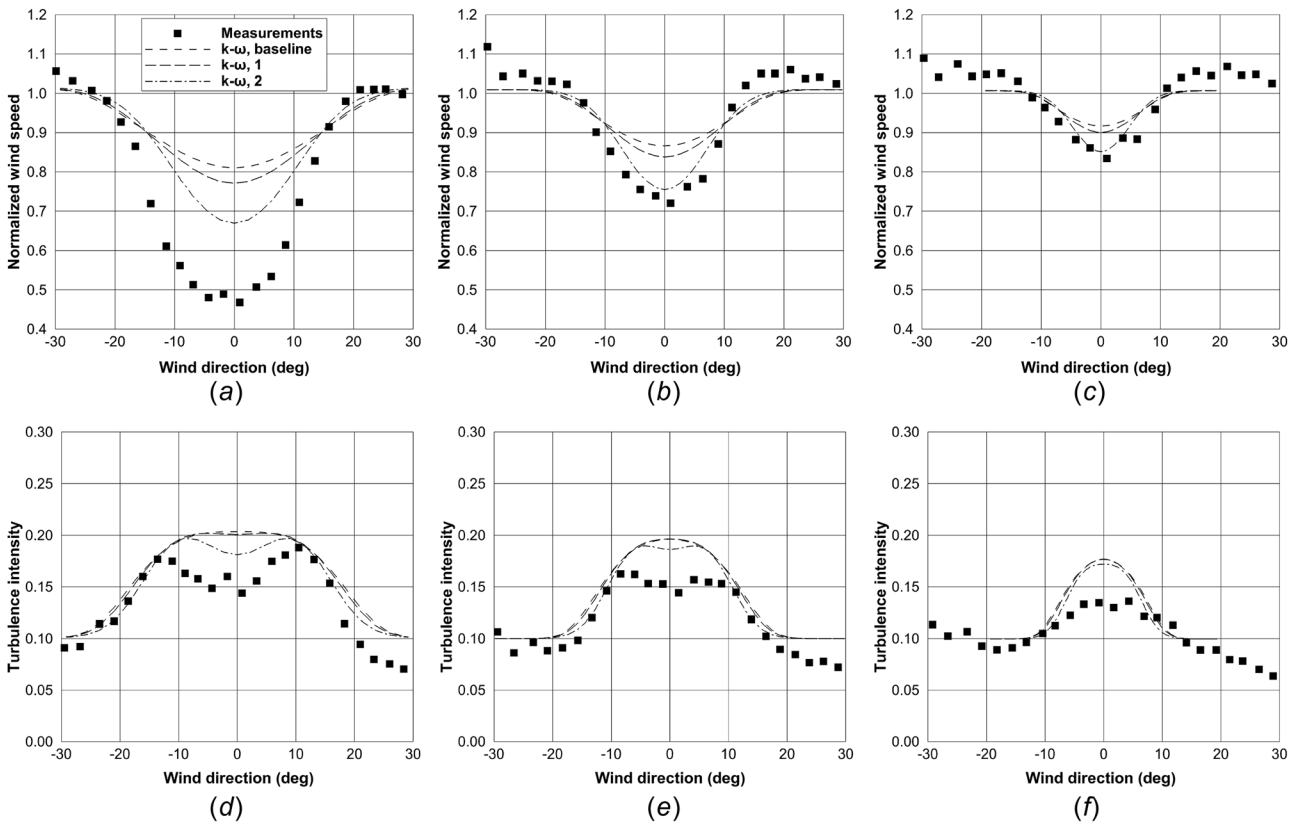

Fig. 8 Wind speed and TI downstream the Nibe wind turbine as a function of wind direction for the k–ω model with the baseline and modified sets of coefficients: (*a*) 2.5*D* downstream, (*b*) 4*D* downstream (*c*) 7.5*D* downstream, (*d*) 2.5*D* downstream, (*e*) 4*D* downstream, and (*f*) 7.5*D* downstream

Downloaded from http://asmedigitalcollection.asme.org/solarenergyengineering/article-pdf/140/3/031007/6330434/sol_140_03_031007.pdf by Stanford University user on 16 August 2021

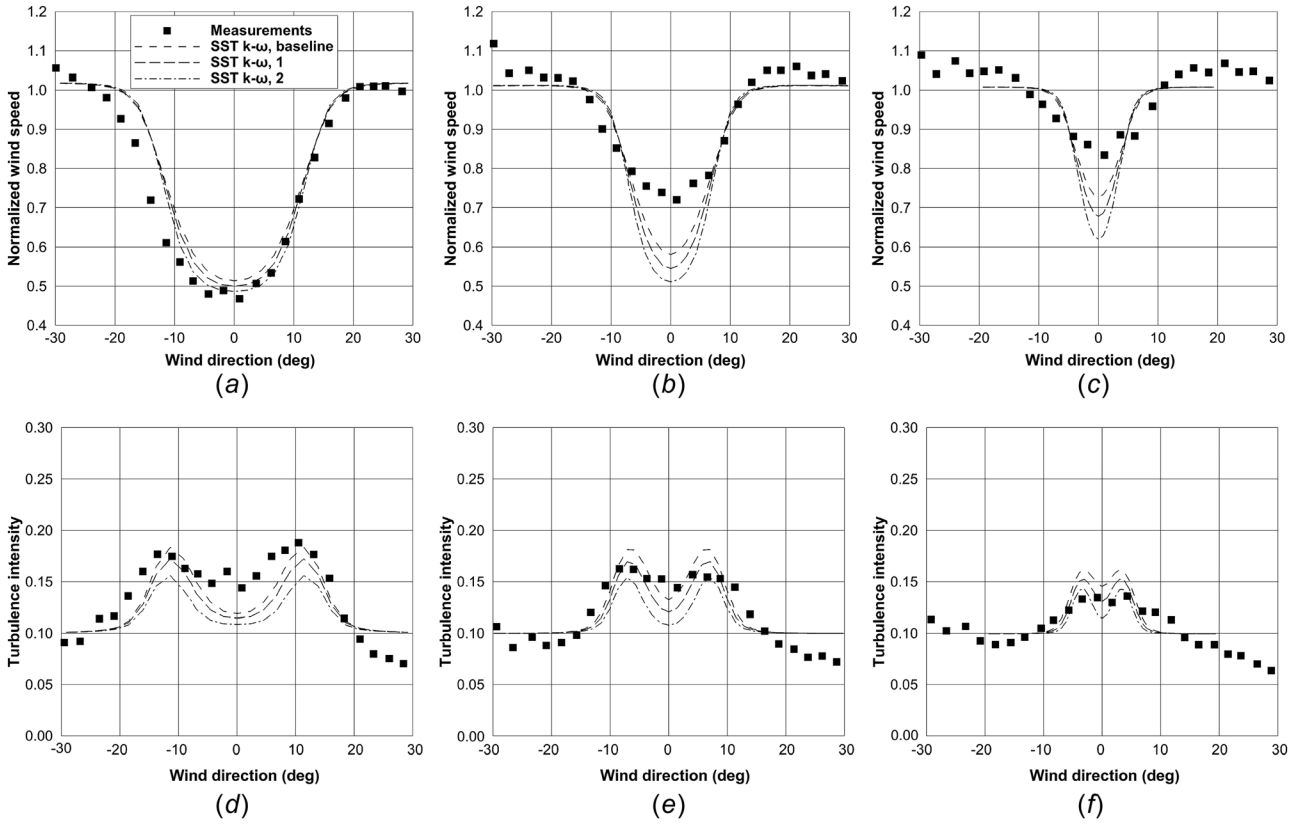

Fig. 9 Wind speed and TI downstream the Nibe wind turbine as a function of wind direction for the *SST k–ω* model with the baseline and modified sets of coefficients: (*a*) 2.5*D* downstream, (*b*) 4*D* downstream, (*c*) 7.5*D* downstream, (*d*) 2.5*D* downstream, (*e*) 4*D* downstream, and (*f*) 7.5*D* downstream

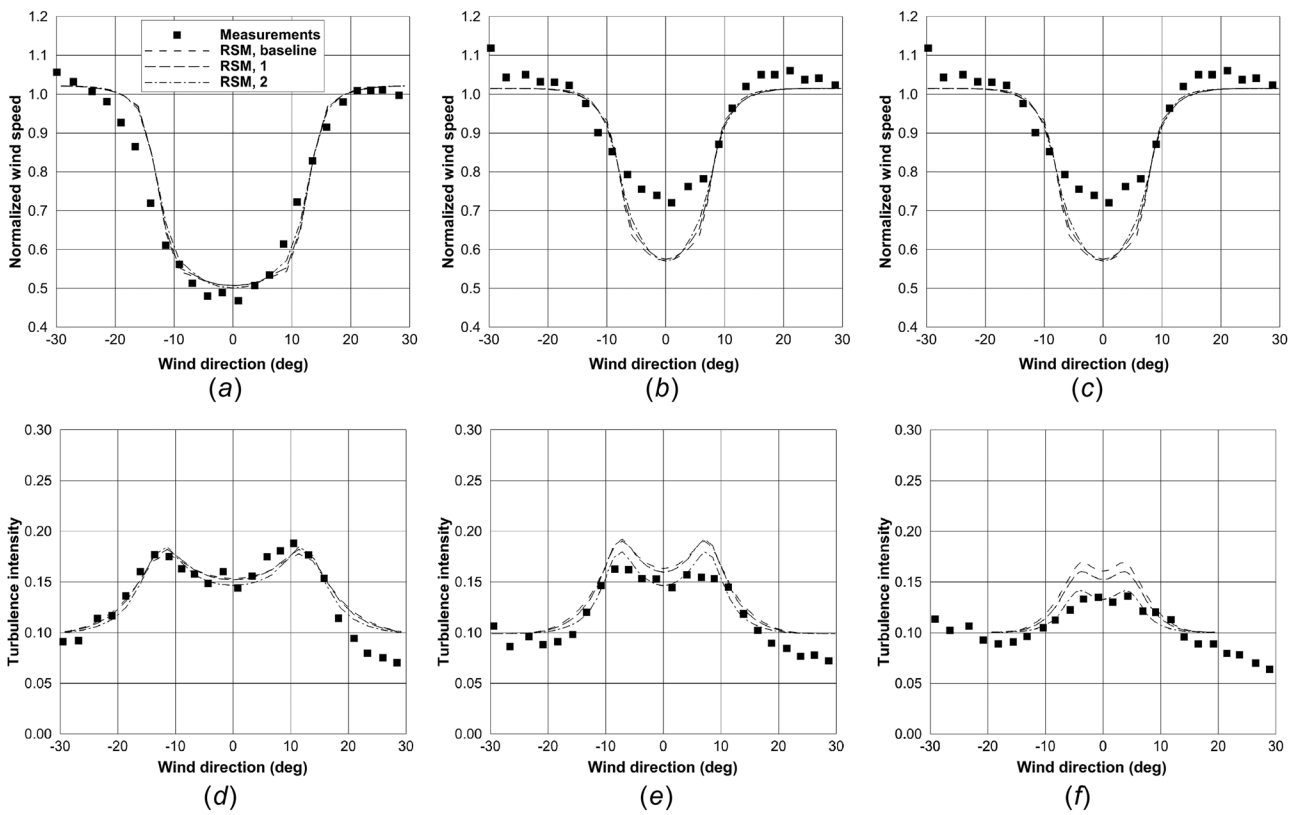

Fig. 10 Wind speed and TI downstream the Nibe wind turbine as a function of wind direction for the RSM with the baseline and modified sets of coefficients: (*a*) 2.5*D* downstream, (*b*) 4*D* downstream, (*c*) 7.5*D* downstream, (*d*) 2.5*D* downstream, (*e*) 4*D* downstream, and (*f*) 7.5*D* downstream

Downloaded from http://asmedigitalcollection.asme.org/solarenergyengineering/article-pdf/140/3/031007/6330434/sol_140_03_031007.pdf by Stanford University user on 16 August 2021

exponent was deleterious on the predictions of the SST k–ω model, especially for the locations at 5.5D and 8D for the Sexbierum case, and 4D and 7.5D for the Nibe case. No significant effect was instead observed for the prediction of the RSM, where the results changed negligibly.

These modified sets of turbulence constants influenced also the turbulence quantities. In particular, it is possible to notice that the predictions of the k–ε and k–ω models were improved with respect to the models using the baseline coefficients: the turbulence kinetic energy in the Sexbierum case and the turbulence intensity in the Nibe case showed the characteristic peaks in the near wake of the wind turbines. Instead, this influence was not beneficial for the SST k–ω model, whose results were more inaccurate. With regard to the RSM, no significant effect was observed as for the wind speed.

7 Conclusions

The present study was conducted in order to compare in a consistent way the principal turbulence models present in literature, namely the k–ε, k–ω, and Reynolds stress model, to introduce the SST k–ω model as an innovative turbulence model for wind turbine simulations, and to investigate and assess the influence of the different turbulence models on the results of the CFD simulations. The turbulence models were implemented in simulations of two stand-alone wind turbines modeled with the constant-distribution actuator disk approach. The wind turbines operated in atmospheric environment which was modeled with the atmospheric surface layer theory. Consistent turbulence model constants for atmospheric surface layer and wake flows were derived according to appropriate experimental observations.

The results showed that the SST k–ω model performed as good as the RSM, which is recognized as the most complete model with general applicability. The results obtained with these two models and with the baseline set of coefficients matched quite accurately the experimental observations both in terms of wind speed and turbulence quantities. On the other hand, the simulations using the k–ε and k–ω models provided poor predictions of wake flows, as already documented in literature.

Modified sets of coefficients were also investigated in order to improve agreement with experimental data. These sets of coefficients improved the predictions of the k–ε and k–ω models, which were, however, not as good as the predictions from the baseline SST k–ω and RSM. The effect of the modified sets of coefficients on these latter models was not effective, and was even deleterious for the SST k–ω.

From the results of this study, it is possible to conclude that the SST k–ω can be used as an effective turbulence model for wind turbine simulations without any particular modification of its coefficients. Its results were showed to be similar to those of the RSM model but obtained at a much faster computation time.

References

[1] Global Wind Energy Council, 2016, "Global Wind Report 2015," Global Wind Energy Council, Brussel, Belgium, Report.

[2] Barthelmie, R. J., Pryor, S. C., Frandsen, S. T., Hansen, K. S., Schepers, J. G., Rados, K., Schlez, W., Neubert, A., Jensen, L. E., and Neckelmann, S., 2010, "Quantifying the Impact of Wind Turbine Wakes on Power Output at Offshore Wind Farms," J. Atmos. Ocean Technol., **27**(8), pp. 1302–1317.

[3] Vermeer, L. J., Sørensen, J. N., and Crespo, A., 2003, "Wind Turbine Wake Aerodynamics," Prog. Aerosp. Sci., **39**(6–7), pp. 467–510.

[4] Crespo, A., Manuel, F., Moreno, D., Fraga, E., and Hernández, J., 1985, "Numerical Analysis of Wind Turbine Wakes," Workshop on Wind Energy Application, Delphi, Greece, May 20–22, pp. 15–25.

[5] Sanderse, B., van der Pijl, S. P., and Koren, B., 2011, "Review of Computational Fluid Dynamics for Wind Turbine Wake Aerodynamics," Wind Energy, **14**(7), pp. 799–819.

[6] Crespo, A., and Hernández, J., 1989, "Numerical Modelling of the Flow Field in a Wind Turbine Wake," Third Joint ASCE/ASME Mechanics Conference, Forum on Turbulent Flows, San Diego, CA, July 9–12, pp. 121–127.

[7] Réthoré, P.-E., 2009, "Wind Turbine Wake in Atmospheric Turbulence," Ph.D. thesis, Aalborg University, Aalborg, Denmark.

[8] Cabezón, D., Migoya, E., and Crespo, A., 2011, "Comparison of Turbulence Models for the Computational Fluid Dynamics Simulation of Wind Turbine Wakes in the Atmospheric Boundary Layer," Wind Energy, **14**(7), pp. 909–921.

[9] Prospathopoulos, J. M., Politis, E. S., and Chaviaropoulos, P. K., 2008, "Modelling Wind Turbine Wakes in Complex Terrain," European Wind Energy Conference and Exhibition, Brussels, Belgium, Mar. 31–Apr. 3, pp. 1–10.

[10] Prospathopoulos, J. M., Politis, E. S., Rados, K. G., and Chaviaropoulos, P. K., 2011, "Evaluation of the Effects of Turbulence Model Enhancements on Wind Turbine Wake Predictions," Wind Energy, **14**(2), pp. 285–300.

[11] El Kasmi, A., and Masson, C., 2008, "An Extended k – ε Model for Turbulent Flow Through Horizontal-Axis Wind Turbines," J. Wind Eng. Ind. Aerodyn., **96**(1), pp. 103–122.

[12] Jones, W. P., and Launder, B. E., 1972, "The Prediction of Laminarization With a Two-Equation Model of Turbulence," Int. J. Heat Mass Transfer, **15**(2), pp. 301–314.

[13] Launder, B. E., and Sharma, B. I., 1974, "Application of the Energy Dissipation Model of Turbulence to the Calculation of Flow Near a Spinning Disc," Lett. Heat Mass Transfer, **1**(2), pp. 131–137.

[14] Pope, S. B., 2000, *Turbulent Flows*, Cambridge University Press, Cambridge, UK.

[15] Wilcox, D. C., 1994, *Turbulence Modeling for CFD*, 2nd ed., DCW Industries, La Cañada, CA.

[16] Wilcox, D. C., 1988, "Reassessment of the Scale-Determining Equation for Advanced Turbulence Models," AIAA J., **26**(11), pp. 1299–1310.

[17] Durbin, P. A., and Pettersson Reif, B. A., 2011, *Statistical Theory and Modeling for Turbulent Flows*, 2nd ed., Wiley, Chichester, UK.

[18] Menter, F. R., 1994, "Two-Equation Eddy-Viscosity Turbulence Models for Engineering Applications," AIAA J., **32**(8), pp. 1598–1605.

[19] Launder, B. E., Reece, G. J., and Rodi, W., 1975, "Progress in the Development of Reynolds-Stress Turbulence Closure," J. Fluid Mech., **68**(3), pp. 537–566.

[20] Speziale, C. B., Sarkar, S., and Gatski, T. B., 1991, "Modelling the Pressure-strain Correlation of Turbulence: An Invariant Dynamical Systems Approach," J. Fluid Mech., **227**(1), pp. 245–272.

[21] Gibson, M. M., and Launder, B. E., 1978, "Ground Effects on Pressure Fluctuations in the Atmospheric Boundary Layer," J. Fluid Mech., **86**(3), pp. 491–511.

[22] Sørensen, J. N., and Myken, A., 1992, "Unsteady Actuator Disc Model for Horizontal Axis Wind Turbines," J. Wind Eng. Ind. Aerodyn., **39**(1–3), pp. 139–149.

[23] Ammara, I., Leclerc, C., and Masson, C., 2002, "A Viscous Three-Dimensional Differential/Actuator-Disk Method for the Aerodynamic Analysis of Wind Farms," ASME J. Sol. Energy Eng., **124**(4), pp. 345–356.

[24] Réthoré, P.-E. M., Sørensen, N. N., Bechmann, A., and Zhale, F., 2009, "Study of the Atmospheric Wake Turbulence of a CFD Actuator Disc Model," European Wind Energy Conference and Exhibition (EWEC), Marseille, France, Mar. 16–19.

[25] Panofsky, H. A., and Dutton, J. A., 1984, *Atmospheric Turbulence: Models and Methods for Engineering Applications*, Wiley, Chichester, UK.

[26] Gryning, S.-E., Batchvarova, E., Brümmer, B., Jørgensen, H., and Larsen, S., 2007, "On the Extension of the Wind Profile Over Homogeneous Terrain Beyond the Surface Boundary Layer," Boundary-Layer Meteorol., **124**(2), pp. 251–268.

[27] Richards, P. J., and Hoxey, R. P., 1993, "Appropriate Boundary Conditions for Computational Wind Engineering Models Using the k-Epsilon Turbulence Model," J. Wind Eng. Ind. Aerodyn., **46–47**, pp. 145–153.

[28] Cleijne, J. W., 1993, "Results of Sexbierum Wind Farm; Single Wake Measurements," TNO Institute of Environmental and Energy Technology, Apeldoorn, The Netherlands, Technical Report No. 93-082.

[29] Taylor, G. J., 1990, "Wake Measurements on the Nibe Wind Turbines in Denmark," National Power—Technology and Environment Center, London, Technical Report No. ETSU WN 5020.

[30] Blocken, B., Stathopoulos, T., and Carmeliet, J., 2007, "CFD Simulation of the Atmospheric Boundary Layer: Wall Function Problems," Atmos. Environ., **41**(2), pp. 238–252.

[31] van der Laan, M. P., Sørensen, N. N., Réthoré, P.-E., Mann, J., Kelly, M. C., Troldborg, N., Schepers, J. G., and Machefaux, E., 2015, "An Improved k–ε Model Applied to a Wind Turbine Wake in Atmospheric Turbulence," Wind Energy, **18**(5), pp. 889–907.

Downloaded from http://asmedigitalcollection.asme.org/solarenergyengineering/article-pdf/140/3/031007/6330434/sol_140_03_031007.pdf by Stanford University user on 16 August 2021